

The interaction of Cl(2 P 3/2) and Cl(2 P 1/2) with nSi(100): Spontaneous etching

W. MüllerMarkgraf and M. J. Rossi

Citation: *Journal of Vacuum Science & Technology A* **9**, 217 (1991); doi: 10.1116/1.577524

View online: <http://dx.doi.org/10.1116/1.577524>

View Table of Contents: <http://scitation.aip.org/content/avs/journal/jvsta/9/2?ver=pdfcov>

Published by the AVS: Science & Technology of Materials, Interfaces, and Processing

Instruments for advanced science

Gas Analysis



- dynamic measurement of reaction gas streams
- catalysis and thermal analysis
- molecular beam studies
- dissolved species probes
- fermentation, environmental and ecological studies

Surface Science



- UHV TPD
- SIMS
- end point detection in ion beam etch
- elemental imaging - surface mapping

Plasma Diagnostics



- plasma source characterization
- etch and deposition process reaction kinetic studies
- analysis of neutral and radical species

Vacuum Analysis




- partial pressure measurement and control of process gases
- reactive sputter process control
- vacuum diagnostics
- vacuum coating process monitoring

contact Hiden Analytical for further details

HIDEN
ANALYTICAL

info@hideninc.com

www.HidenAnalytical.com

CLICK to view our product catalogue 

The interaction of $\text{Cl}(^2P_{3/2})$ and $\text{Cl}(^2P_{1/2})$ with $n\text{-Si}(100)$: Spontaneous etching

W. Müller-Markgraf^{a)} and M. J. Rossi

Department of Chemical Kinetics, SRI International, Menlo Park, California 94025

(Received 8 August 1990; accepted 3 November 1990)

The sticking coefficient γ of ground-state Cl ($\text{Cl}(^2P_{3/2})$) and spin-orbit excited Cl^* ($\text{Cl}(^2P_{1/2})$) on lightly doped $n\text{-Si}(100)$ was measured using resonance-enhanced multiphoton ionization of Cl and Cl^* at mTorr pressure in a Knudsen cell. For Cl only an upper limit of $\gamma \leq 5 \times 10^{-5}$ could be obtained and for Cl^* $\gamma = 4.6 \times 10^{-4}$ was measured. These γ values are temperature independent in the range of 300–600 K and the sum corresponds to a spontaneous etch rate of 9.4 Å/min for $\text{Si}(100)$. SiCl_2 was the principal etch product under these spontaneous etch conditions, and no SiCl_4 was found over the given temperature range.

I. INTRODUCTION

The interaction of neutral transient species (i.e., atoms and free radicals), with surfaces is widely believed to be of prime importance in electronic materials processing such as plasma etching, as well as in thermal and nonthermal deposition processes. Most processing techniques use electrical discharges of gaseous media, which undergo decomposition into ionic and neutral atomic and molecular fragment species that impinge on the material of interest. However, the active transients involved in etching and deposition in such processing systems are mainly thought to be the neutral atoms and free radicals, although energetic ion bombardment assists many chemical processes, either in the gas phase or on the surface. In fact, the role of energetic ion bombardment is apparent in situations where one obtains anisotropic (directional) etch profiles (reactive ion etching) or subsurface accumulation of etch gases in the solid sample. In the practice of electronic materials processing it is often difficult to unambiguously separate the effects due to neutral and charged species because both types of species contribute towards the processing of the material at hand. Therefore, the method of choice for the characterization and study of these two differing mechanisms is to perform laboratory experiments where only one type of transient species is generated to interact with the material of interest.

The present study aims at understanding that portion of the etch mechanism of single crystal silicon in a chlorine atmosphere which is supported by neutral transient species in what has been called spontaneous etching. It is a fundamental study of the kinetics and reaction products of atomic chlorine in its ground and spin-orbit excited states, namely $\text{Cl}(^2P_{3/2})$ and $\text{Cl}(^2P_{1/2})$ (or Cl^*), with the $n\text{-Si}(100)$ surface. Our goal is to understand the etch mechanism from a fundamental point of view. The gas-surface interaction of Cl or Cl^* with the solid Si surface is the first step.

Because of the technological importance of Cl-containing discharges, much basic research has been conducted to investigate the etching of single-crystal silicon by Cl_2 .¹⁻⁷ Below 425 K there is no detectable reaction, whereas stable etching products such as SiCl_4 and SiCl_2 are detected above 425 K. Many ultrahigh vacuum (UHV) studies involving the interaction of Si with Cl_2 have focused on ion-assisted etching, whose effects on the identity and distribution of the

stable etch products are still a matter of debate.

On the other hand, detailed studies of Cl atoms with polycrystalline⁸ or single-crystal silicon⁹ surfaces under well-defined experimental conditions are scarce. Because Cl_2 is inert toward Si in the absence of ion bombardment and at low temperatures, the active etchant in plasma processing of Si with Cl-containing gases must include atomic Cl as far as spontaneous etching is concerned. On the other hand, in most plasma etchers the Si surface is exposed to the plasma to a varying degree, and therefore ion-assisted etching will dominate as evidenced by the anisotropy obtained. In a recent study Chuang and Coburn showed that molecular Cl_2 etches Si only under Ar^+ bombardment.¹⁰ This result is consistent with the statement about the inertness of Cl_2 and the activity of atomic Cl in that—prior to etching—molecular adsorbed Cl_2 is dissociated by energetic Ar^+ into atoms which subsequently engage in Si etching. Therefore, fundamental experiments on the Si/Cl system have been undertaken in which a quantifiable atomic Cl density has been obtained in a radio frequency⁸ or microwave discharge⁹ and subsequently been observed to interact with the solid surface.

Another practical method of obtaining a controlled atmosphere of atomic Cl is the high-power excimer laser photolysis of Cl_2 . Kinetic studies have appeared in the literature in which Cl atoms were generated using 308-nm excimer laser radiation in the presence of doped or undoped single-crystal surfaces.^{11,12} The role of photodissociation of Cl_2 by 308 nm radiation, as well as etching under continuous irradiation, has been reported and discussed.¹³⁻¹⁵ Photoinduced desorption of reaction products in the silicon-chlorine etching system has been studied using time-of-flight mass spectrometry under UHV conditions as a probe for the progress of the etching reaction.^{16,17} A systematic comparison of 248 with 193-nm excimer laser-induced etching of p -type $\text{Si}(100)$ revealed considerable mechanistic differences in the etch mechanism between the two irradiation frequencies. This study also clarified the role of free atomic Cl generated in a microwave discharge in its interaction with the silicon surface with and without concurrent UV irradiation of the surface.¹⁸

It is instructive to consider the relative reactivity of Cl_2 and Cl on a silicon surface at the same temperature to appreciate the role of free atomic Cl in discharges affecting the

spontaneous etch rate of single crystal silicon. Using Flamm's data⁹ for etching a n -type doped Si(100) sample at 500 K at a doping level of $\sim 5 \times 10^{19}$ P/cm³, we calculate a relative etch efficiency ratio of 4.4 logarithmic units in favor of atomic Cl. As a result of Flamm's work, we know that both the crystallographic face of Si and the doping level influence the etch rate in a major way. For the above example, we used 1000 Å/min mTorr for the etch rate of Si at 500 K and the cited doping level. We present here our own data on the rate and stable reaction products of spontaneous Si etching monitored by the disappearance of atomic Cl and Cl^* using the laser-based technique of resonance-enhanced multiphoton ionization (REMPI).

II. EXPERIMENTAL

The experimental apparatus and technique have been described in detail elsewhere,¹⁹ so only a brief description is given here. The principle of the measurement consists of determining the lifetime of Cl and Cl^* in the presence of the single-crystal Si surface under total pressure conditions that heavily favor gas-wall collisions over gas-gas collisions. Figure 1 presents a schematic of the experimental apparatus, and Table I provides a list of the relevant low-pressure reactor parameters. The Si surface is housed in a Knudsen cell probed by both REMPI and modulated molecular beam mass spectrometry (MBMS). In the absence of any gettering of Cl by the Si surface, the lifetime of Cl in the Knudsen cell is given by its escape rate constant through the escape aperture. All internal surfaces of the Knudsen cell, with the exception of the sample (Si) surface, are passivated against Cl attack by a Teflon coating, so the measured escape rate

TABLE I. Low-pressure reactor parameters.

VLPR reactor ^a characteristics	
Knudsen reactor volume	487 cm ³
Test (sample) surface area (active surface)	14.5 cm ²
Test surface temperature	295–750 K
Peak total pressure, pulsed mode	$\sim 1.2 \times 10^{-3}$ Torr
Peak number density, Cl atoms/pulse	$\sim 10^{13}$ molecules cm ⁻³ ^b
Collision frequency, reactor walls	$5320 \times (T/M)^{1/2}$ s ⁻¹
Collision frequency, test surface	$109 \times (T/M)^{1/2}$ s ⁻¹
Escape aperture diameter/length	3/3 mm
Escape rate constant	$0.319 \times (T/M)^{1/2}$ s ⁻¹ ^c
Pulsed chlorine atom source ^d	
Pulse width (solenoid valve)	300 μ s or 50–300 ms ^d
Pulse repetition rate (typ.),	
"long" pulse mode (50–300 ms)	0.1 s ⁻¹
Cl ₂ decomposition (typ.),	
solenoid valve permanently open	$\sim 40\%$ ^e
Cl ₂ decomposition (typ.),	
"long" pulse mode (10 ms)	$\sim 25\%$ ^e

^a Reactor and atom source coated with Teflon.

^b Estimated from steady-state precursor flow rate and observed fractional depletion of Cl₂ under typical experimental conditions.

^c Calibrated with Cl₂. Calculated value: $k_{\text{esc}} = 0.355 \times (T/M)^{1/2}$ with a Clausing's factor of 0.67, according to aperture length/diameter = 1.0.

^d Depending on operation mode; short pulse, long pulse.

^e Reference 19.

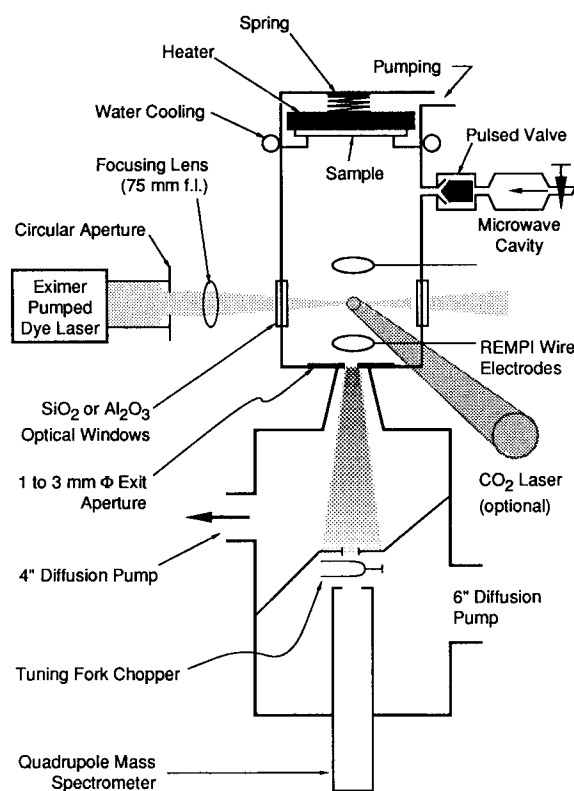


FIG. 1. Schematic of the experimental configuration.

constant is determined entirely by the geometrical parameters of the Knudsen cell. Any decrease in Cl lifetime upon introduction of the sample surface is attributed to chemical interaction of Cl with that sample surface. Because the gas-wall collision frequency of any species with the test surface can be calculated from the geometrical parameters of the Knudsen cell, the sticking coefficient of Cl and Cl^* on the Si surface can be determined using the measured rate constant for loss of Cl, Cl^* on the test surface.

A pulsed Cl source is necessary for kinetic experiments. To this end, a pulsed solenoid valve (General Valve, Inc.) was carefully passivated using the above-mentioned Teflon coating so that a substantial fraction of the Cl and Cl^* atoms generated from a microwave discharge in Cl₂ or CF₃Cl survived the expansion into the Knudsen cell. After the pulsed valve was opened for a few tens of milliseconds, pulsed ex-cimer laser-pumped dye laser radiation was used to interrogate the Cl and Cl^* density at a probe pulse repetition frequency of 20–50 Hz, providing up to 100 data points on the Cl decay curve. The pulse repetition frequency for the Cl bursts was usually 0.2 Hz for the REMPI measurements, whereas the MBMS results were obtained with the valve continuously open to give a continuous flux of Cl and Cl^* .

Combining REMPI diagnostics with MBMS made it possible to calibrate the REMPI signal by measuring the decrease in the (calibrated) mass spectrometric precursor signal (i.e., at $m/e = 70$ for Cl₂). When the microwave discharge (Evenson cavity) was turned on, this decrease in the MBMS signal was related to the REMPI signal at $t = 0$, the time corresponding to the closure of the pulsed valve,

thus establishing a 1:1 correlation between precursor molecules lost (MBMS signal) and Cl atoms generated (REMPI signal). Even though all the REMPI decays for both Cl and Cl* were simple exponentials, we measured the peak density of Cl and Cl* to develop a quantitative grasp of the unimolecular decay kinetics. An initial density of up to 10^{13} Cl atoms/cm³ was routinely achieved. The details of calibrating of the escape rate constant, the REMPI spectrum for Cl and Cl* and the REMPI signal processing are described in another report.¹⁹

The sample surface was a 2 in. diam, 0.5-mm-thick *n*-type Si(100) wafer ($3 \Omega \text{ cm}$, doping level $1.5 \times 10^{15} \text{ cm}^{-3}$) cleaned in "piranha" solution,²⁰ a sequential peroxide solution for chemical oxidation, followed by an aqueous HF etching. After profusely rinsing the wafer with deionized water we immediately mounted it on the heater assembly in the Knudsen cell and pumped it to a base pressure of 10^{-8} Torr. We assumed that the surface was hydrogen terminated,²¹ because no induction period in the evolution of stable etch products was ever observed.

III. RESULTS AND DISCUSSION

The temporal decay of both the Cl and Cl* REMPI signal in an all-Teflon-lined Knudsen cell (no Si surface present) follows simple exponential decay kinetics, with the decay time constant corresponding to the escape rate constant of Cl at 300 K (Table I).¹⁹ This finding means that the chemical interaction of Cl with the Teflon liner (probed at 404 nm) and the quenching of Cl* by the Teflon walls (probed at 405.3 nm) is unimportant during the lifetime of Cl, Cl* in the low-pressure reactor, even in the presence of comparable amounts of Cl₂. This situation is a good starting point for our investigations because no corrections need to be made to allow for a "background" reaction of Cl and Cl* with the large internal surface of the Knudsen cell reactor.

Cl and Cl* REMPI profiles, observed in experiments with the *n*-Si(100) wafer in place, show single exponential decays with apparent rate constants very close to the escape rate constant of Cl. No apparent saturation behavior upon repeated exposure of the Si surface to Cl and Cl* was observed. The REMPI signal decays were identical from Cl pulse to pulse, a fact that allowed us to superimpose many Cl decays, thereby achieving a meaningful statistical data analysis. Kinetic experiments (i.e., Cl and Cl* lifetime measurements), were conducted in the temperature range of 298 to 670 K (wafer temperature).

As an example, an experiment at 304 K is shown in Fig. 2. The escape rate constant has been calibrated in every individual experiment using the mass spectrometer for direct measurement of the Cl₂ escape rate. We therefore compare the decay rates of the Cl REMPI signal [Fig. 2(a)] and the Cl* signal [Fig. 2(b)] with the Cl escape rate [$k_{\text{esc}}(\text{Cl}, 295 \text{ K}) = 0.925 \text{ s}^{-1}$]. Analysis of the data shown in Fig. 2 yields $k_{\text{decay}} = 0.955 \pm 0.025 \text{ s}^{-1}$ for Cl, which is identical to k_{esc} within experimental error. We conclude that the amount of Cl lost on the Si wafer is too small to be resolved in the current experiment.

We define a sticking or "uptake" coefficient γ as the ratio k_s/ω , where k_s is the measured loss rate constant of Cl or Cl*

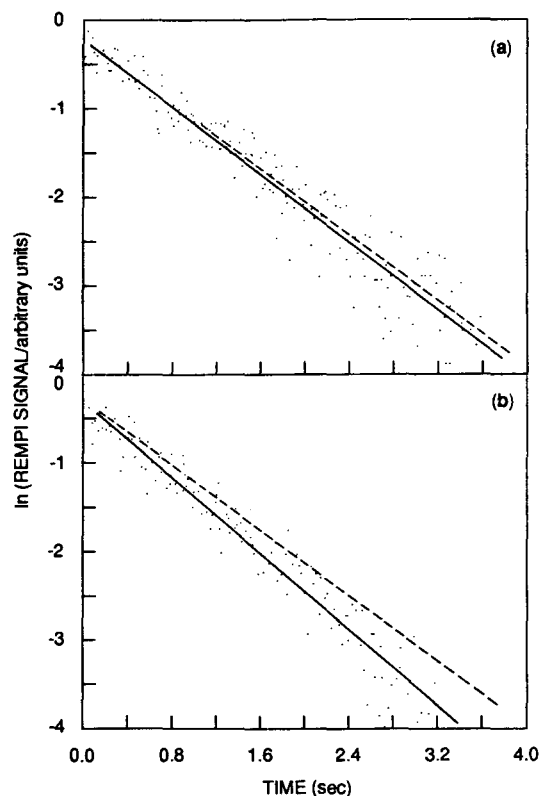


FIG. 2. REMPI time profiles taken at 404 nm [(a) Cl $^2P_{3/2}$] and 405.3 nm [(b) Cl $^2P_{1/2}$] in the presence of *n*-doped Si(100) wafer. $T(\text{wafer}) = 304 \text{ K}$, dashed line = escape rate.

on the Si surface and ω is the calculated collision frequency for the sample surface (Table I). This ratio describes the fractional collision rate leading to irreversible loss of Cl or Cl* from the gas phase and the uptake kinetics of Cl regardless of the fate of Cl on the Si surface (physisorption, chemisorption, surface reaction). The current experiment on Cl/Si leads to an upper limit of

$$\gamma(\text{Cl}, 304 \text{ K}) \leq 5 \times 10^{-5}$$

with $k_s \leq 0.025 \text{ s}^{-1}$ corresponding to the error limit of k_{decay} . While monitoring the Cl* REMPI signal we encountered a situation shown in Fig. 2 with an apparent decay rate constant of $1.07 \pm 0.02 \text{ s}^{-1}$. This value, although close to that of $k_{\text{esc}}(\text{Cl})$, was nevertheless significantly faster. Assuming a greater precision for the *in situ* calibration of k_{esc} than for the actual REMPI measurement of the decay rate constant, we obtained

$$k_s(\text{Cl}^*, 304 \text{ K}) = 0.145 \pm 0.02 \text{ s}^{-1}$$

for the rate constant for irreversible removal of Cl* from the gas phase in the presence of the silicon wafer, regardless of the subsequent fate of Cl on the Si surface. This translated into

$$\gamma(\text{Cl}^*, 304 \text{ K}) = (4.6 \pm 0.6) \times 10^{-4}$$

Analysis of experiments conducted at 597 K wafer temperature, but with ambient temperature reactor walls, yielded

$$\gamma(\text{Cl}^*, 597 \text{ K}) = (2.7 \pm 1.7) \times 10^{-4}$$

which was not significantly different from the ambient tem-

perature value. The Cl ground-state REMPI signal profile at 597 K again did not show a statistically significant deviation from k_{esc} , so the upper limit for $\gamma(\text{Cl}, 304 \text{ K})$ given above also applies to 597 K.

At this point it seems useful to include an estimate of the rate of spontaneous etching by Cl* relative to a typical ion-assisted etching rate obtained either in a plasma etcher under realistic conditions or from laboratory experiments. The gas-surface impingement rate (flux) for one mTorr of Cl* atoms is calculated as 3.4×10^{17} molecules $\text{cm}^{-2} \text{s}^{-1}$. We assume that it takes two reactive collisions by Cl* to lead to the observed stable etch product SiCl₂, and we ignore the contribution of Cl in view of its small uptake coefficient. This leads us to a spontaneous etching rate of 7.9×10^{13} atoms/s cm^2 per mTorr of Cl* which translates into a linear etch rate of 9.4 Å/min.

In comparison a polysilicon thin film in a LAM Research single wafer etcher is etched at a rate of 4000–5000 Å/min at 250 W at 100–900 mTorr of Cl₂ in He with 10% SF₆.²² In another experiment a single crystal (100) or (111) Si wafer was subjected to reactive ion-beam etching using Cl₂ from a Kaufman ion gun at 0.5 mA/cm². At 400 eV ion energy the measured Si etch rate was 400 Å/min, and at 800 eV the rate was 1200 Å/min.²³ Following a plasma beam study of single crystal Si etching we estimate an etch rate of 1800 Å/min at an impingement rate of 4×10^{18} Cl₂ molecules corresponding to a density of about 15 mTorr and 400 eV sample bias.¹ In another ion beam study serving as a simulation of plasma-assisted etching, an etch rate of 215 Å/min was measured at a Cl atom flux of 1.2×10^{17} molecules $\text{cm}^{-2} \text{s}^{-1}$, a flux very similar to our experimental situation (see above). In this experiment an Ar⁺ beam impinged on a chlorine covered Si surface at 600 eV.²⁴ These few examples show that the spontaneous etch rate of single crystal Si by Cl* is smaller by two orders of magnitude on the average, depending on the experimental circumstances of the plasma-assisted etching experiment. However, the spontaneous etching rate albeit small is observable under our experimental conditions at variance with the results of Chuang and Coburn.¹⁰

We did not observe any incubation saturation or passivation effects in the lifetime of Cl* or Cl exposed to *n*-Si(100), even after prolonged exposure to the Cl/Cl* ambient. Because Cl* was found to have a small but finite γ on *n*-Si(100), we attempted to observe etch products leaving the surface continuously as Cl* was irreversibly removed from the gas phase. For this experiment, the Si wafer was exposed to a steady-state flow of Cl and Cl* for 2 h by leaving the pulsed valve continuously open. Figure 3 shows the thermal desorption of an etch product monitored at $m/e = 63$ (SiCl⁺). Immediately after the Cl, Cl* flow was turned off, evolution of the mass spectrometric signal at $m/e = 63$ was observed as the wafer was heated up. There was no detectable etch product and hence no background signal in the gas phase after the chlorine flow was turned off and before heating. Figure 3 shows a large flux of the etch product off the Si surface at near to ambient temperature, and a similar, but smaller product desorption signal can be seen at a higher temperature, starting around 500 K. Extensive reference experiments with Cl₂ exposed to *n*-Si(100) revealed that Cl₂

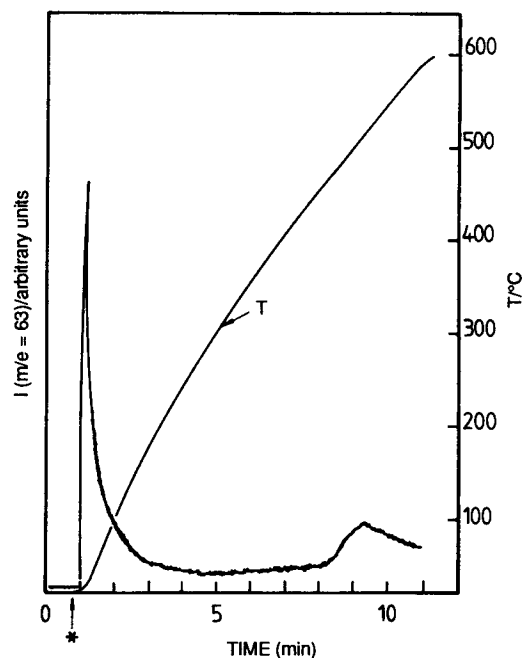


Fig. 3. Thermal desorption of the etch product of the Cl/Cl*/*n*-Si(100) reaction, observed at $m/e = 63$ (SiCl⁺). The wafer ($T = 295 \text{ K}$) was exposed to a steady-state flow of Cl/Cl* for two hours. Then the flow was turned off at $t = 0$. Temperature ramp was started at (*). No product was observed in the absence of Cl atoms (discharge off).

did not interact with silicon, hence did not result in any detectable etch product. Furthermore, Cl₂ did not deactivate Cl*, at least up to densities of 1.5×10^{13} molecules cm^{-3} .

Using a conservative value for the sum of the Cl and Cl* density of 5×10^{12} molecules/cm³, we calculated the impingement rate (flux) for Cl and Cl* on the Si surface as $5.4 \times 10^{16} \text{ s}^{-1} \text{ cm}^{-2}$. After 2 h and using a conservative value $\gamma = 5 \times 10^{-6}$ for both Cl and Cl*, we calculate a deposited chlorine adlayer of 2×10^{15} molecules/cm² representing a lower limit. Typical values for both Cl and Cl* densities and the corresponding γ values are larger by a factor of 5. The conclusion is that at least one monolayer of Cl and probably a multilayer was deposited under the above experimental conditions. The results of Fig. 3 suggest that the low-temperature desorption peak is related to the presence of a Cl-containing multilayer, whereas the high-temperature desorption feature corresponds to the destruction of the last Cl-containing adlayer at the Si/Cl interface.

A similar but smaller product desorption signal could be observed at $m/e = 98$ (SiCl₂⁺), but no SiCl₃⁺ signal could be detected even after a prolonged search. We conclude, therefore, that the etch product is SiCl₂ and that SiCl₄ is not a detectable etch product under our etching conditions. We do not expect significant amounts of SiCl to survive the many gas-wall collisions inside the low pressure reactor due to its high reactivity.²⁵ However, we cannot unambiguously decide whether SiCl₂ is the product of the interaction between Si(100) with Cl or Cl*. In view of the small spin-orbit splitting in chlorine (881 cm^{-1}), we assume that Si etching is brought about by both chlorine species because of the strong Si-Cl bond (114 kcal/mol or $\sim 5 \text{ eV}$ for gas-phase

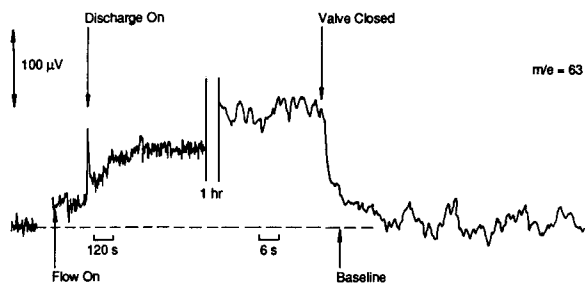


FIG. 4. Product formation during a typical preparation of a thermal desorption experiment, as shown in Fig. 3, observed at $m/e = 63$. Wafer temperature, 295 K; $F^i(\text{Cl}_2) = 5 \times 10^{15}$ molecules s^{-1} ; Cl_2 decomposition $\sim 30\%$.

SiCl_2). Another observation in support of participation of both chlorine species in spontaneous Si etching is the apparent insensitivity of the observed etch rates to the condition of the microwave discharge, which can control the relative density of Cl and Cl^* as monitored by the REMPI signal by up to a factor of 4 in either direction for a total range of a factor of 16.

We also observed a mass spectroscopic signal for SiCl_2 in a steady-state experiment while the Si wafer was exposed to a continuous flow of Cl and Cl^* . Figure 4 shows the mass spectrometric signal at $m/e = 63$ recorded during preparation of the thermal desorption experiment described above (Fig. 3). When a flow of Cl_2/He [$F^i(\text{Cl}_2) = 5 \times 10^{15}$ molecules s^{-1}] is allowed to enter the Knudsen cell (pulsed valve open continuously; no microwave discharge), a small unidentified background signal is observed. After the microwave discharge is ignited, the SiCl_2 flux originating from the Si surface approaches a steady-state value, which is, however, small compared to the product flux obtained in the thermal desorption experiment shown in Fig. 3. The signal drops to the baseline on a time scale of several seconds when the Cl/ Cl^* flow is stopped by closing the valve. This surface coverage represents the surface condition of the Si sample immediately before the start of the thermal desorption experiment (Fig. 3).

The identity of the etch products resulting from chlorine attack on solid Si seems to vary significantly depending on the experimental conditions. Madix and Schwarz observed the evolution of SiCl_2 when they exposed single crystal Si to Cl_2 at temperatures exceeding 1000 K in ultrahigh vacuum.²⁶ In a recent detailed UHV study Jackman, Ebert, and Foord observed two stable phases as a result of Cl_2 interaction with (100) Si. The β phase easily saturates at a monolayer, has a high binding energy to the underlying Si and evolves a mixture of SiCl_2 and SiCl_4 upon thermal desorption. The less strongly bound α phase is a multilayer corrosion phase sitting atop the β phase and releases SiCl_4 exclusively.²⁷

More importantly, these authors could show that a competing reaction occurred under steady state exposure to Cl_2 releasing SiCl_4 independent of the population of the two stable adsorbate phases. Once the Cl_2 exposure stopped, the steady state generation of SiCl_4 ceased and the two stable adsorbate phases could be analyzed. The relationship be-

tween these two competing surface mechanisms is obviously complex and remains obscure. In the present example the answer obtained under UHV conditions may not be at all representative of the relevant etching reactions observed under a higher pressure of the etch gas as is common in electronic materials processing. What is needed are real-time *in situ* measurements of surface processes performed under the relevant experimental conditions.

Another example of differing results achieved under vastly different experimental conditions contrasting "surface science" against materials technology is illustrated by the magnitude of the sticking coefficients of Cl and Cl_2 on (100) or (111) Si. In this case, however, the differences can be explained in terms of the differing surface coverage of the material at hand. Jackman and co-workers measure $\gamma(\text{Cl}_2, 300 \text{ K}) \geq 0.13$ on atomically clean Si.²⁷ They claim that the Cl_2 beam is attenuated by 50% and 70% at 300 and $\geq 900 \text{ K}$, respectively, and the "absorbed" chlorine is partitioned in some way between the α and β phases discussed above and the steady state SiCl_4 observed in their experiment. Other workers found similar numbers in that exposure of Cl_2 to an atomically clean Si surface leads to rapid formation of a monolayer of adsorbed Cl atoms with a sticking coefficient of 0.1.²⁸ Upon further Cl_2 dosing γ of Cl_2 on Si drops rapidly to less than 0.01.²⁹ The same situation also seems to hold for Cu etching by Cl_2 .³⁰

The conclusion concerning the identity of the etch product can be compared with the etch product distribution in "chemical sputtering" experiments (ion-assisted etching), in which the SiCl_x distribution once more seems to be very sensitive to experimental conditions, notably the ion energy.³¹ On the other hand, an *in situ* investigation of plasma-etch products of polysilicon by Fourier transform IR (FTIR) analysis essentially revealed only SiCl_4 .⁸ In the chemical and ion-assisted etching of Si by Cl_2 , SiCl_4 seems to be the primary species leaving the surface at processing temperatures, with SiCl_2 favored at temperatures above 800 K. The result of the present work as far as the identity of the major etch product is concerned, is at variance with the conclusion^{8,27} that unsaturated silicon species appear as products only when physically sputtered from the surface.

Sesselmann *et al.*¹⁸ found that Cl_2 etching leads to the buildup of a passivating surface layer of SiCl_x with $x < 1$ that strongly impedes further reaction for $x > 0.5$. This passivating layer causes negligible subsurface penetration by Cl_2 because dissociative chemisorption of Cl_2 on top of the SiCl_x monolayer is no longer a rapid process. However, when atomic chlorine is the chlorinating agent, higher degrees of surface chlorination are achieved, thus effectively bypassing the rate-limiting step of dissociative chemisorption in the case of Cl_2 chlorination. Thus, chlorination with atomic Cl leads to higher rates and chlorination efficiencies compared with those of Cl_2 . Despite the fact that chlorination by atomic Cl is a fast and efficient process, Chuang and Coburn¹⁰ did not observe spontaneous etching of n -type Si(111) by Cl in their single-collision molecular beam-surface experiment, perhaps because their observation time was not adequate to measure the rate or the product spectrum of the spontaneous etching of Si by atomic Cl.

IV. CONCLUSIONS

The present work conclusively shows that atomic chlorine in its upper spin state ($^2P_{1/2}$) spontaneously etches $n\text{-Si}(100)$ in the absence of ion bombardment or energetic radiation at a rate of $9.4 \text{ \AA}/\text{min}$. This etch rate is approximately two orders of magnitude lower than typical plasma etch rates. Under steady state pressure conditions of approximately 1 mTorr of Cl and Cl_2 (ratio of Cl to Cl_2 density $\sim 1:2$) or equivalently, a chlorine flux of $\sim 3.5 \times 10^{17} \text{ cm}^{-2} \text{ s}^{-1}$, the atomic sticking coefficient was measured to be $\gamma(\text{Cl}, 300 \text{ K}) \leq 5 \times 10^{-5}$ and $\gamma(\text{Cl}^*, 300 \text{ K}) = 4.6 \times 10^{-4}$. These values are temperature independent in the range of 300–600 K. The primary etch product observed was SiCl_2 which could be desorbed in multilayer quantities after steady state exposure of Si to a mixture of Cl and Cl_2 . This situation is similar to the one found in a UHV Si etching study by molecular Cl_2 ,²⁷ in which a multilayer corrosion phase (α) with similar desorption characteristics was found. However, it evolved as SiCl_4 at variance with our result.

ACKNOWLEDGMENT

W. M.-M. wishes to thank the Deutsche Forschungsgemeinschaft for a grant.

^{a1} Postdoctoral Research Associate. Present address: Linde AG, Werksgruppe TVT, D-8000 München 71, Germany.

¹ D. L. Smith and P. G. Saviano, *J. Vac. Sci. Technol.* **21**, 768 (1982).

² D. L. Smith and R. H. Bruce, *J. Electrochem. Soc.* **129**, 2045 (1982).

³ S. C. McNevin and G. E. Becker, *J. Vac. Sci. Technol. B* **3**, 485 (1985).

⁴ A. W. Kofschoten, R. A. Haring, and A. E. deVries, *J. Appl. Phys.* **55**, 3813 (1984).

⁵ F. H. M. Sanders, A. W. Kofschoten, J. Dieleman, R. A. Haring, A. Haring, and A. E. deVries, *J. Vac. Sci. Technol. A* **2**, 487 (1984).

⁶ R. A. Rossen and H. H. Sawin, *J. Vac. Sci. Technol. A* **5**, 1595 (1987).

⁷ J. Dieleman, F. H. M. Sanders, A. W. Kofschoten, P. C. Zalm, A. E. deVries, and A. Haring, *J. Vac. Sci. Technol. B* **3**, 1384 (1985).

⁸ T. A. Cleland and D. W. Hess, *J. Vac. Sci. Technol. B* **7**, 35 (1989).

⁹ E. A. Ogryzlo, D. E. Ibbotson, D. L. Flamm, and J. A. Mucha, *J. Appl. Phys.* **67**, 3115 (1990).

¹⁰ Mei-Chen Chuang and J. W. Coburn, *J. Vac. Sci. Technol. A* **3**, 1969, (1990).

¹¹ T. Arikado, M. Sekine, H. Okano, and Y. Horiike, *Mater. Res. Soc. Proc.* **29**, 167 (1984).

¹² Y. Horiike, N. Hayasaka, M. Sekine, T. Arikado, M. Nakase, and H. Okano, *Appl. Phys. A* **44**, 313 (1987).

¹³ R. Kullmer and D. Bäuerle, *Appl. Phys. A* **43**, 227 (1987).

¹⁴ P. Mogyorosi, K. Piglmayer, R. Kullmer, and D. Bäuerle, *Appl. Phys. A* **45**, 293 (1988).

¹⁵ R. Kullmer and D. Bäuerle, *Appl. Phys. A* **47**, 377 (1988).

¹⁶ T. S. Baller, D. J. Oostra, A. E. deVries, and G. N. A. van Veen, *J. Appl. Phys.* **60**, 2321 (1986).

¹⁷ Y.-L. Li, Z.-J. Zhang, Q.-K. Zheng, Z.-K. Wu, and Q.-Z. Qin, *Appl. Phys. Lett.* **53**, 792 (1989).

¹⁸ W. Sesselmann, E. Hudeczek and F. Bachmann, *J. Vac. Sci. Technol. B* **7**, 1284 (1989).

¹⁹ W. Müller-Markgraf and M. J. Rossi, *Rev. Sci. Instrum.* **61**, 1217 (1990).

²⁰ W. Kern, *Semicond. Int.* 94 (April 1984); *W. Kern, RCA Eng.* **28-4**, 99 (1983).

²¹ V. A. Burrows, Y. J. Chabal, G. S. Higashi, K. Raghavachari, and S. B. Christman, *Appl. Phys. Lett.* **53**, 998 (1988).

²² J. Herrmann, LAM Research Corporation, Fremont, CA.

²³ P. K. Charvat, E. E. Krueger and A. L. Ruoff, *J. Vac. Sci. Technol. B* **4**, 812 (1986).

²⁴ T. M. Mayer and R. A. Barker, *J. Vac. Sci. Technol.* **21**, 757 (1982).

²⁵ J. B. Jeffries, *Mat. Res. Soc. Proc.* **117**, 41 (1988).

²⁶ R. J. Madix and J. A. Schwarz, *Surf. Sci.* **24**, 264 (1971).

²⁷ R. B. Jackman, H. Ebert and J. S. Foord, *Surf. Sci.* **176**, 183, (1986).

²⁸ P. K. Larsen, N. V. Smith, M. Schlueter, H. H. Farrell, K. M. Ho, and M. L. Cohen, *Phys. Rev. B* **17**, 2612 (1978).

²⁹ J. V. Florio and W. D. Robertson, *Surf. Sci.* **18**, 398 (1969).

³⁰ D. Westphal and A. Goldmann, *Surf. Sci.* **131**, 113 (1983).

³¹ D. J. Oostra, A. Haring, R. P. van Ingen, and A. E. deVries, *J. Appl. Phys.* **64**, 315 (1988).